Prediction of Peak Internal Fields in Direct-Coupled-Cavity Filters

Christoph Ernst, *Associate Member, IEEE*, and Vasil Postoyalko, *Member, IEEE*

***Abstract*—In this paper, an explicit expression of the peak electric-field strength in the cavities of Chebyshev direct-coupled-cavity waveguide filters is derived. It is shown that the electric-field strength can be predicted from the analysis of the time-averaged stored energy in the lumped low-pass prototype, from which the cavity filter was derived. This simplifies the analysis and study of the power-handling capability of these types of filters considerably, as the stored energy in the prototype filters is easily computed. The analysis of the field distribution in the cavities of an example third-degree Chebyshev direct-coupled-cavity filter shows that the explicit expression for the peak electric-field strength derived in this paper agrees closely with results obtained from a TE_{10} circuit model of the filter, from a full-wave electromagnetic solver and from measurements.**

***Index Terms*—Direct-coupled-cavity filters, electric-field strength, power-handling capability, stored energy.**

I. Introduction

PEAK internal fields are an important consideration when the power-handling capability of a filter is evaluated. Dielectric breakdown and multipaction breakdown is a direct consequence of the large buildup of the electric fields in electrical filters [1]–[5]. Young proposed an approximate approach to the prediction of the peak internal fields in direct-coupled filters [6]. He related the ratio of the maximum to midband equivalent power ratio to the ratio of the maximum to the midband group delay. This necessitated the introduction of a safety factor, which he suggested "*[. . .] is probably always less than 2*." No justification is given other than the consideration of several examples. However, results recently obtained for highly selective filters [7]–[10] show that a much larger safety factor can be required for these types of filters.

In this paper, a new approach for developing an explicit expression for the peak internal fields in cavity filters is presented. This approach is based on the consideration of the distribution of the time-averaged stored energy (t.a.s.e.) in the filter. In [11]–[13], the relationship between group delay and t.a.s.e. in a filter is rigorously derived. This makes it possible to relate the distribution of energy in a lumped low-pass prototype filter to the distribution of energy in a coupled resonator filter, which is derived from the prototype by means of a frequency transformation. Using these ideas in this paper, an accurate and explicit expression for the peak electric fields is derived for Chebyshev direct-coupled-cavity waveguide filters. It is shown that the peak electric fields can be related directly to the peak t.a.s.e. in the elements of the lumped prototype filter, from which the cavity filter was derived.

This paper considerably simplifies the analysis and study of the power-handling capability of these types of filters [1], [14], [6], [15]. Only the stored energy distribution in the lumped low-pass prototype needs to be computed and the peak t.a.s.e. has been tabulated for lumped prototype filters of degrees 1–15 and return loss of 15, 20, and 25 dB.

This paper also gives a justification for the implicit assumptions made in [7]–[9], and [13], where the power-handling capability of some Butterworth, Chebyshev, and general Chebyshev cavity filters are analyzed and compared with each other by considering solely the stored energy distributions in lumped low-pass prototype filters.

II. Prediction of the Electric-Field Strength

Rectangular waveguide TE_{10} mode filters with bandwidths of up to 20% can be designed from lumped low-pass prototype filters using the approximate frequency transformation in [16] and [17], i.e.,

$$T_{L\to WG}\colon \omega \to \alpha \cdot \sin\left(\beta_{10}(\omega)\ell\right). \tag{1}$$

Equating α and ℓ [16], [17] by solving

$$1 = \alpha \sin\left(\frac{2\pi}{\lambda_{g,\,hi}}\,\ell\right) \tag{2}$$

and

$$-1 = \alpha \sin\left(\frac{2\pi}{\lambda_{g,\,lo}}\,\ell\right) \tag{3}$$

gives

$$\frac{1}{\alpha} = \sin\left(2\pi \frac{\lambda_{g,\,lo}}{\lambda_{g,\,lo}+\lambda_{g,\,hi}}\right) < 0 \tag{4}$$

$$\ell = \frac{\lambda_{g,\,hi}\lambda_{g,\,lo}}{\lambda_{g,\,lo}+\lambda_{g,\,hi}} \tag{5}$$

where

$$\lambda_{g,\,lo} \quad \text{guide wavelength at lower band-edge } f_{\mathrm{lo}} \tag{6}$$

$$\lambda_{g,\,hi} \quad \text{guide wavelength at upper band-edge } f_{\mathrm{hi}} \tag{7}$$

$$\beta_{10} = \sqrt{\omega^2\mu\epsilon - \left(\frac{\pi}{a}\right)^2} \tag{8}$$

$$f_c \quad \text{cutoff frequency of } \mathrm{TE}_{10} \text{ mode} \tag{9}$$

$$a \quad \text{width of waveguide} \tag{10}$$

$$b \quad \text{height of waveguide.} \tag{11}$$

Manuscript received May 13, 2001; revised December 13, 2001. This work was supported by Filtronic plc.

C. Ernst was with the School of Electronic and Electrical Engineering, The University of Leeds, Leeds LS2 9JT, U.K. He is now with Lorch Microwave, Salisbury, MD 21801 USA (e-mail: c_ernst@ieee.org).

V. Postoyalko is with the School of Electronic and Electrical Engineering, The University of Leeds, Leeds LS2 9JT, U.K.

Digital Object Identifier 10.1109/TMTT.2002.806906

Making use of the results in [13, eq. (46)],

$$W_{\mathrm{WG}} = W_{\mathrm{LP}}\big(T(\omega)\big) \cdot \frac{dT(\omega)}{d\omega} \tag{12}$$

the stored energy (W_{WG}) in the cavities of a narrow-band waveguide filter can be related to the stored energy (W_{LP}) in the low-pass prototype for frequencies for which the frequency transformation T is valid, i.e., for frequencies close to the resonance frequencies of the cavities. As the field distribution is well known at the frequency when the cavity becomes resonant, the stored energy can then be related to the electric-field strength at the centers of the cavities.

Hence, consider the electromagnetic (EM) field distribution in a waveguide cavity of length ℓ for frequencies ω close to the resonance frequency ω_0, i.e., when $\beta_{10} \approx 2\pi/\lambda_{g0}$ and where λ_{g0} is the resonance wavelength. The field distribution is closely approximated by the field distribution of a perfect standing TE_{10} wave, i.e.,

$$\mathbf{E}_y(\omega, x, z) = \sin\frac{\pi x}{a}\,\mathbf{E}_0 \sin\big(\beta_{10}(\omega)z\big) \tag{13}$$

$$\mathbf{H}_z(\omega, x, z) = \frac{-\pi/a}{j\omega\mu}\cos\frac{\pi x}{a}\,\mathbf{E}_0 \sin\big(\beta_{10}(\omega)z\big) \tag{14}$$

$$\mathbf{H}_x(\omega, x, z) = \frac{-j\beta_{10}(\omega)}{\omega\mu}\sin\frac{\pi x}{a}\,\mathbf{E}_0 \cos\big(\beta_{10}(\omega)z\big) \tag{15}$$

with a maximum electric-field strength of $|\mathbf{E}_0|$. In the case of direct-coupled-cavity filters, further evidence of this field distribution can be found in [18], where the voltage distributions in numerous TEM direct-coupled-cavity filters have been computed from the chain matrix analysis. In the case of general-coupled cavity filters, it may be pointed out that Rhodes [17] implicitly assumed the field distribution in (13)–(15) when he derived the design equations, which have been successfully used in practice, for this type of filter.

The stored energy is then obtained by integrating the dot product of the electric fields and the dot product of the magnetic fields over the cavity volume [19], i.e.,

$$\tilde{W}_{\mathrm{av}} = \frac{1}{4}\int_0^{\ell}\int_0^{b}\int_0^{a}\left[\epsilon\vec{\mathbf{E}}\cdot\vec{\mathbf{E}}^* + \mu\vec{\mathbf{H}}\cdot\vec{\mathbf{H}}^*\right] dx\,dy\,dz \tag{16}$$

and after substituting for $\mathbf{E}$ and $\mathbf{H}$ using (13)–(15)

$$\tilde{W}_{\mathrm{av}} = |\mathbf{E}_0|^2 \cdot \frac{ab}{8} \cdot \ell \cdot \epsilon. \tag{17}$$

On the other hand, the stored energy in a cavity can also be computed from the low-pass prototype using (12) and expressing the t.a.s.e. in the cavity filter in terms of port equivalent voltages and currents. Two equations for the stored energy are obtained. Combining these two equations, the electric field in the waveguide cavity can be directly related to the stored energy in the lumped low-pass prototype.

A. Stored Energy in the Waveguide Cavities Estimated From the Corresponding Lumped Low-Pass Prototype

In order to obtain an equation of the stored energy in terms of port equivalent voltages and currents, the following alternative expression of the stored energy is employed, which can be derived from a variational theorem [13], [20], [19], i.e.:

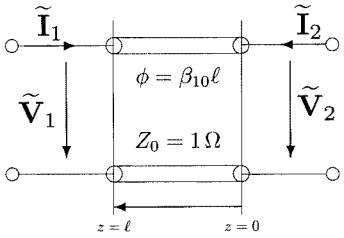

Fig. 1. Distributed transmission-line model of a TE_{10} mode propagating in a section of rectangular waveguide of length ℓ.

$$\tilde{W}_{\mathrm{av}} = \frac{j}{4}\sum_{r=1}^{2}\left[\oint_{S_r}\left(\vec{\mathbf{E}}_r \times \frac{d\vec{\mathbf{H}}_r^*}{d\omega} + \frac{d\vec{\mathbf{E}}_r^*}{d\omega}\times\vec{\mathbf{H}}_r\right)\cdot\vec{u}_n\,ds\right. \tag{18}$$

where S_r is the terminal surface of port r and $\vec{u}_n$ is a unity vector normal to the terminal surface. Following Schwinger and Saxon [20] and choosing the reference planes of a passive lossless two-port at $z = 0$ and $z = \ell$, and assuming that no evanescent modes are present, (18) reduces to

$$\tilde{W}_{\mathrm{av}} = \frac{j}{4}\int_0^{a}\int_0^{b}\sum_{r=1}^{2}\left(-\mathbf{E}_{y,r}\left[\frac{\partial\mathbf{H}_{x,r}}{\partial\omega}\right]^* - \mathbf{H}_{x,r}\left[\frac{\partial\mathbf{E}_{y,r}}{\partial\omega}\right]^*\right) dy\,dx \tag{19}$$

where $\mathbf{E}_{y,1}$, $\mathbf{H}_{x,1}$ and $\mathbf{E}_{y,2}$, $\mathbf{H}_{x,2}$ are the corresponding transverse electric field and transverse magnetic field of the dominant TE_{10} mode at the port reference planes. Defining equivalent port voltages $\tilde{\mathbf{V}}_r(\omega)$ and equivalent port currents $\tilde{\mathbf{I}}_r(\omega)$ of the waveguide system corresponding to the equivalent transmission-line model in Fig. 1, i.e.,

$$\mathbf{E}_y = \sin\frac{\pi x}{a}\sqrt{\frac{2}{ab}\frac{\omega\mu}{\beta_{10}}}\,\tilde{\mathbf{V}}(z,\omega) \tag{20}$$

$$\mathbf{H}_z = \frac{-\pi/a}{j\omega\mu}\cos\frac{\pi x}{a}\sqrt{\frac{2}{ab}\frac{\omega\mu}{\beta_{10}}}\,\tilde{\mathbf{V}}(z,\omega) \tag{21}$$

$$\mathbf{H}_x = \frac{-\beta_{10}}{\omega\mu}\sin\frac{\pi x}{a}\sqrt{\frac{2}{ab}\frac{\omega\mu}{\beta_{10}}}\,\tilde{\mathbf{I}}(z,\omega) \tag{22}$$

and substituting the above into (19), the stored energy in the waveguide section is obtained in terms of the equivalent port voltages $\tilde{\mathbf{V}}_1(\omega)$, $\tilde{\mathbf{V}}_2(\omega)$, and the equivalent port currents $\tilde{\mathbf{I}}_1(\omega)$, $\tilde{\mathbf{I}}_2(\omega)$, i.e.,

$$\begin{aligned}\tilde{W}_{\mathrm{av}}(\omega) &= \frac{j}{4}\frac{ab}{2}\sum_{r=1}^{2}\left(\frac{2}{ab}\left[\tilde{\mathbf{V}}_r(\omega)\frac{d\tilde{\mathbf{I}}_r(\omega)^*}{d\omega} + \tilde{\mathbf{I}}_r(\omega)\frac{d\tilde{\mathbf{V}}_r(\omega)^*}{d\omega}\right]\right.\\ &\quad + \frac{(\pi/a)^2}{ab\omega\beta_{10}^2}\left\{\tilde{\mathbf{V}}_r(\omega)^*\tilde{\mathbf{I}}_r(\omega) - \tilde{\mathbf{V}}_r(\omega)\tilde{\mathbf{I}}_r(\omega)^*\right\}\Bigg).\end{aligned} \tag{23}$$

Note that the equivalent voltages and currents have been marked with a tilde in order to distinguish them from the voltages and currents in the lumped low-pass prototype filter. Hence, treating each cavity of a waveguide filter as a two-port extending from

$z = 0$ to $z = \ell$, the t.a.s.e. in the waveguide cavity can be calculated from the equivalent transmission-line circuit model. Note that the t.a.s.e. obtained in this way is an approximate value since the t.a.s.e. in the evanescent modes excited by the coupling apertures at the reference planes have been neglected. This corresponds to modeling the coupling apertures by ideal impedance inverters.

The term $\tilde{\mathbf{V}}_r(\omega)^*\tilde{\mathbf{I}}_r(\omega) - \tilde{\mathbf{V}}_r(\omega)\tilde{\mathbf{I}}_r(\omega)^*$ in (23) is proportional to $W_{\mathrm{av},m} - W_{\mathrm{av},e}$ [19]. Hence, it can be neglected for frequencies close to the resonance frequency of the cavity.

Employing the frequency transformation in (1), the voltages and currents in the lumped low-pass prototype are related to the voltages and currents in the transmission-line prototype filter by

$$\tilde{\mathbf{V}}_r(\omega) = \mathbf{V}_r\big(T(\omega)\big) \text{ and } \tilde{\mathbf{I}}_r(\omega) = \mathbf{I}_r\big(T(\omega)\big). \tag{24}$$

When these expressions for the voltages and currents in the transmission-line prototype are substituted into (23), the term in square brackets in (23) can be written as

$$\frac{4}{j} W_{\mathrm{av}}\big(T(\omega)\big) \frac{dT(\omega)}{d\omega} \tag{25}$$

i.e., the stored energy in the lumped low-pass prototype times the derivative of the frequency transformation. Using the expression for the phase constant (8) and the frequency transformation (1), the derivative of the frequency transformation can be evaluated, i.e.,

$$\frac{dT}{d\omega} = \frac{\omega\mu\epsilon}{\beta_{10}}|\alpha|\ell\cos\left(\beta_{10}\ell\right). \tag{26}$$

Hence, neglecting the term $\tilde{\mathbf{V}}_r(\omega)^*\tilde{\mathbf{I}}_r(\omega) - \tilde{\mathbf{V}}_r(\omega)\tilde{\mathbf{I}}_r(\omega)^*$ in (23) and using (25) for the term in square brackets in (23), as well as the relation in (26), the stored energy in a waveguide cavity ($\tilde{W}_{\mathrm{av}}$) is approximately related to the stored energy (W_{av}) in the corresponding section of the lumped low-pass prototype by

$$\tilde{W}_{\mathrm{av}}(\omega) \approx W_{\mathrm{av}}(T(\omega))\ell|\alpha|\cos(\beta_{10}\ell)\frac{\omega\mu\epsilon}{\beta_{10}} \tag{27}$$

for frequencies close to resonance, i.e., for frequencies around the center frequency of the passband.

B. Peak Electric-Field Strength

The maximum electric-field strength in a cavity can now be obtained for frequencies close to the resonance frequency of the cavity combining (17) and (27), i.e.,

$$|\mathbf{E}_0|^2 \approx \frac{8}{ab}|\alpha|\cos\left(\beta_{10}\ell\right)\frac{\omega\mu}{\beta_{10}} W_{\mathrm{av}}\big(T(\omega)\big). \tag{28}$$

In order to be able to compute the peak amplitude

$$\mathbf{E}_{\max} = \max\left\{\,|\mathbf{E}_0|\,,\, 0 \le \omega < \infty\right\} \tag{29}$$

it is necessary to solve

$$\frac{d\,|\mathbf{E}_0|}{d\omega} = 0 \tag{30}$$

for ω in order to obtain the frequency at which the amplitude of the electric field becomes a maximum. Due to the fundamental relation between stored energy, group delay, and selectivity [10]–[13], [21], [22], large peak stored energies occur for frequencies in the stopband or passband close to the band edges for reasonable selective minimum phase filters. Hence, it is reasonable to evaluate (28) either at the lower or at the upper band edge. The term $\omega\mu/\beta_{10}$ in (28) is always larger at the lower band edge than at the upper band edge, which suggests to evaluate (28) at the lower band edge. Alternatively, if the peak frequencies in the lumped low-pass filter are known, the frequency transformation in (1) may be used to calculate the approximate peak frequencies in the waveguide filter on the lower side of the passband. Also, from Fig. 2, the magnitude of the scaling factor α is much greater than unity for filters with a fractional bandwidth of 20% and smaller. Using (3), we thus have

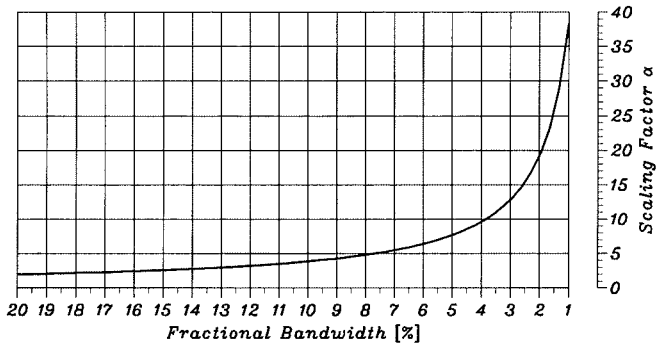

Fig. 2. Magnitude of the scaling factor α in waveguide filters with a passband center frequency of $f_{\mathrm{center}} = 1.586\,f_c$.

$$\frac{-1}{\alpha} = \sin\left(\frac{2\pi}{\lambda_{g,\,lo}}\,\ell\right) \approx \beta_{10}(f_{\mathrm{lo}})\ell. \tag{31}$$

Hence, the cos-term in (28) can be replaced by $\cos(1/\alpha)$ without introducing a large error. The negative sign has been dropped since cos is an even function. Concerning the stored energy $W_{\mathrm{av},k}$ in the kth element in the lumped low-pass filter, its maximum value may be taken. Hence, the peak electric-field strength in the kth cavity is approximately given by

$$\mathbf{E}_{\max,k} \approx \sqrt{\frac{8}{ab}|\alpha|\cos\left(\frac{1}{\alpha}\right)\sqrt{\frac{\mu}{\epsilon}}\frac{1}{\sqrt{1-\left(\dfrac{f_c}{f_{\mathrm{lo}}}\right)^2}}\max\{W_{\mathrm{av},k}\}} \tag{32}$$

and $\max\{W_{\mathrm{av},k}\}$ is the maximum stored energy in the kth element of the corresponding lumped low-pass prototype filter. In Tables I–III, the peak t.a.s.e. in lumped low-pass prototype filters of degree 1–15 and return loss of 15, 20, and 25 dB have been listed for future reference covering commonly used Chebyshev filters.

III. Comparison of Predicted and Computed Peak Electric-Field Strength

Employing Rhodes' [22] very accurate explicit design equations, the peak electric-field strength in a large number of Chebyshev transmission-line prototype filters of different degrees and bandwidths up to $\Delta_{\mathrm{BW}} = 20\%$ was computed and compared to the predicted ones employing (32). For filters of

TABLE I
t.a.s.e. IN CHEBYCHEV LUMPED-ELEMENT LOW-PASS PROTOTYPE FILTERS WITH 15-dB MINIMUM PASSBAND RETURN LOSS ($P_A = 1$ W)

Peak t.a.s.e. in *Joule*, $W_{av,k}^{(max)} = \max\{W_{av,k}(\omega), \omega \in [0,\infty[\}$ $(k = 1 \cdots 15)$, in lumped element Chebychev low-pass prototype filters ($P_A = 1W$).

degree	element 1	element 2	element 3	element 4	element 5	element 6	element 7	element 8	element 9	element 10	element 11	element 12	element 13	element 14	element 15	total t.a.s.e.	average t.a.s.e.	LTA ratio
1	0.1807															0.1807	0.1807	1.0000
2	0.6854	0.4651														1.0711	0.5355	1.2797
3	1.1476	1.2848	0.5596													2.7405	0.9135	1.4065
4	1.5110	2.0241	1.5301	0.5977												5.1313	1.2828	1.5778
5	1.7869	2.6985	2.3777	1.6606	0.6164											8.2247	1.6449	1.6405
6	1.9943	3.3063	3.1612	2.5849	1.7392	0.6268										12.0142	2.0024	1.6512
7	2.1502	3.8487	3.8951	3.4339	2.7246	1.7903	0.6332									16.4970	2.3567	1.6528
8	2.2672	4.3299	4.5827	4.2343	3.6256	2.8249	1.8253	0.6373								21.6717	2.7090	1.6917
9	2.3550	4.7554	5.2250	4.9955	4.4734	3.7707	2.8997	1.8503	0.6402							27.5378	3.0598	1.7076
10	2.4206	5.1311	5.8231	5.7209	5.2824	4.6581	3.8845	2.9570	1.8687	0.6423						34.0949	3.4095	1.7079
11	2.4695	5.4626	6.3789	6.4119	6.0592	5.5044	4.8071	3.9758	3.0018	1.8827	0.6438					41.3428	3.7584	1.7060
12	2.5057	5.7551	6.8945	7.0693	6.8066	6.3186	5.6856	4.9302	4.0502	3.0375	1.8935	0.6450				49.2814	4.1068	1.7214
13	2.5322	6.0131	7.3721	7.6938	7.5261	7.1054	6.5306	5.8378	5.0335	4.1117	3.0663	1.9020	0.6459			57.9106	4.4547	1.7271
14	2.5515	6.2408	7.8143	8.2863	8.2185	7.8673	7.3482	6.7099	5.9678	5.1210	4.1629	3.0899	1.9089	0.6466		67.2303	4.8022	1.7255
15	2.5654	6.4417	8.2235	8.8480	8.8843	8.6056	8.1421	7.5538	6.8647	6.0800	5.1958	4.2061	3.1094	1.9145	0.6472	77.2405	5.1494	1.7253

Angular frequency, $\omega_{av,k}^{(max)}$ $(k = 1 \cdots 15)$, of the peak t.a.s.e. in lumped element Chebychev low-pass prototype filters.

degree	element 1	element 2	element 3	element 4	element 5	element 6	element 7	element 8	element 9	element 10	element 11	element 12	element 13	element 14	element 15	total t.a.s.e.
1	0.0000															0.0000
2	1.4383	-														1.2263
3	1.3033	1.0720	-													1.1375
4	1.2132	1.0891	1.0078	-												1.0850
5	1.1597	1.0780	1.0324	0.9920	-											1.0567
6	1.1258	1.0655	1.0355	1.0117	0.9883	-										1.0403
7	1.1031	1.0552	1.0336	1.0175	1.0029	0.9882	-									1.0300
8	1.0870	1.0470	1.0304	1.0187	1.0087	0.9989	0.9891	-								1.0232
9	1.0754	1.0406	1.0272	1.0183	1.0109	1.0040	0.9971	0.9903	-							1.0184
10	1.0666	1.0355	1.0244	1.0172	1.0115	1.0063	1.0013	0.9963	0.9914	-						1.0150
11	1.0599	1.0314	1.0219	1.0160	1.0114	1.0073	1.0036	0.9998	0.9961	0.9925	-					1.0124
12	1.0548	1.0281	1.0198	1.0148	1.0110	1.0077	1.0047	1.0018	0.9990	0.9961	0.9934	-				1.0105
13	1.0507	1.0253	1.0179	1.0136	1.0104	1.0077	1.0053	1.0030	1.0007	0.9985	0.9962	0.9941	-			1.0089
14	1.0475	1.0230	1.0164	1.0126	1.0098	1.0075	1.0055	1.0036	1.0018	1.0000	0.9982	0.9964	0.9948	-		1.0077
15	1.0450	1.0210	1.0150	1.0116	1.0092	1.0073	1.0056	1.0040	1.0025	1.0010	0.9996	0.9981	0.9966	0.9953	-	1.0067

Tolerance $< 1 * 10^{-4}$; LTA ratio: Largest to Average Ratio

TABLE II
t.a.s.e. IN CHEBYCHEV LUMPED-ELEMENT LOW-PASS PROTOTYPE FILTERS WITH 20-dB MINIMUM PASSBAND RETURN LOSS ($P_A = 1$ W)

Peak t.a.s.e. in *Joule*, $W_{av,k}^{(max)} = \max\{W_{av,k}(\omega), \omega \in [0,\infty[\}$ $(k = 1 \cdots 15)$, in lumped element Chebychev low-pass prototype filters ($P_A = 1W$).

degree	element 1	element 2	element 3	element 4	element 5	element 6	element 7	element 8	element 9	element 10	element 11	element 12	element 13	element 14	element 15	total t.a.s.e.	average t.a.s.e.	LTA ratio
1	0.1005															0.1005	0.1005	1.0000
2	0.5112	0.3333														0.7828	0.3914	1.3060
3	0.9387	1.0180	0.4267													2.1643	0.7214	1.4112
4	1.2809	1.7044	1.2237	0.4666												4.1848	1.0462	1.6291
5	1.5335	2.3558	1.9842	1.3306	0.4866											6.8170	1.3634	1.7279
6	1.7132	2.9490	2.7233	2.1351	1.3946	0.4979										10.0499	1.6750	1.7606
7	1.8384	3.4755	3.4340	2.9127	2.2336	1.4364	0.5049									13.8786	1.9827	1.7530
8	1.9240	3.9353	4.1079	3.6704	3.0377	2.3039	1.4652	0.5094								18.3009	2.2876	1.7957
9	1.9815	4.3325	4.7391	4.4059	3.8214	3.1304	2.3566	1.4859	0.5126							23.3155	2.5906	1.8293
10	2.0193	4.6731	5.3251	5.1153	4.5879	3.9331	3.2031	2.3973	1.5012	0.5149						28.9218	2.8922	1.8412
11	2.0437	4.9635	5.8652	5.7949	5.3365	4.7193	4.0224	3.2619	2.4295	1.5130	0.5166					35.1193	3.1927	1.8371
12	2.0593	5.2100	6.3603	6.4425	6.0649	5.4908	4.8237	4.0965	3.3105	2.4553	1.5221	0.5179				41.9079	3.4923	1.8448
13	2.0692	5.4183	6.8123	7.0565	6.7711	6.2473	5.6111	4.9110	4.1593	3.3511	2.4764	1.5294	0.5189			49.2873	3.7913	1.8612
14	2.0756	5.5936	7.2236	7.6364	7.4531	6.9875	6.3857	5.7110	4.9861	4.2132	3.3854	2.4939	1.5352	0.5197		57.2575	4.0898	1.8672
15	2.0798	5.7406	7.5968	8.1823	8.1095	7.7100	7.1475	6.4990	5.7972	5.0517	4.2599	3.4146	2.5085	1.5400	0.5204	65.8183	4.3879	1.8648

Angular frequency, $\omega_{av,k}^{(max)}$ $(k = 1 \cdots 15)$, of the peak t.a.s.e. in lumped element Chebychev low-pass prototype filters.

degree	element 1	element 2	element 3	element 4	element 5	element 6	element 7	element 8	element 9	element 10	element 11	element 12	element 13	element 14	element 15	total t.a.s.e.
1	0.0000															0.0000
2	1.8532	-														1.5544
3	1.5210	1.1985	-													1.2950
4	1.3512	1.1785	1.0659	-												1.1757
5	1.2584	1.1428	1.0804	1.0237	-											1.1155
6	1.2026	1.1149	1.0736	1.0410	1.0074	-										1.0814
7	1.1665	1.0944	1.0642	1.0424	1.0222	1.0004	-									1.0603
8	1.1419	1.0792	1.0557	1.0397	1.0259	1.0124	0.9974	-								1.0464
9	1.1248	1.0677	1.0485	1.0361	1.0260	1.0165	1.0068	0.9961	-							1.0368
10	1.1125	1.0589	1.0425	1.0325	1.0247	1.0177	1.0108	1.0036	0.9956	-						1.0299
11	1.1038	1.0519	1.0377	1.0293	1.0230	1.0175	1.0123	1.0071	1.0016	0.9956	-					1.0248
12	1.0975	1.0463	1.0336	1.0265	1.0212	1.0168	1.0127	1.0088	1.0047	1.0004	0.9957	-				1.0208
13	1.0930	1.0417	1.0303	1.0240	1.0195	1.0159	1.0126	1.0095	1.0063	1.0031	0.9996	0.9959	-			1.0178
14	1.0898	1.0380	1.0274	1.0219	1.0180	1.0149	1.0121	1.0096	1.0071	1.0046	1.0019	0.9991	0.9962	-		1.0154
15	1.0876	1.0349	1.0250	1.0201	1.0166	1.0139	1.0116	1.0095	1.0074	1.0054	1.0033	1.0012	0.9988	0.9964	-	1.0134

Tolerance $< 1 * 10^{-4}$; LTA ratio: Largest to Average Ratio

degree 3 or larger, the predicted peak electric-field strength by (32) always agreed within 10% with the computed one.

For a series of low-degree Chebyshev transmission-line prototype filters of fractional bandwidths between

TABLE III
t.a.s.e. IN CHEBYCHEV LUMPED-ELEMENT LOW-PASS PROTOTYPE FILTERS WITH 25-dB MINIMUM PASSBAND RETURN LOSS ($P_A = 1$ W)

Peak t.a.s.e. in *Joule*, $W_{av,k}^{(max)} = \max\{W_{av,k}(\omega), \omega \in [0,\infty[\}$ $(k = 1 \cdots 15)$, in lumped element Chebychev low-pass prototype filters ($P_A = 1\,W$).

degree	element 1	element 2	element 3	element 4	element 5	element 6	element 7	element 8	element 9	element 10	element 11	element 12	element 13	element 14	element 15	total t.a.s.	average t.a.s.	LTA ratio
1	0.0563															0.0563	0.0563	1.0000
2	0.3831	0.2441														0.5800	0.2900	1.3210
3	0.7709	0.8245	0.3352													1.7421	0.5807	1.4199
4	1.0906	1.4608	1.0102	0.3767												3.4903	0.8726	1.6741
5	1.3222	2.0862	1.7039	1.1051	0.3980											5.7906	1.1581	1.8014
6	1.4793	2.6613	2.4058	1.8250	1.1612	0.4103										8.6271	1.4379	1.8509
7	1.5810	3.1684	3.0949	2.5497	1.9004	1.1976	0.4179									11.9926	1.7132	1.8494
8	1.6444	3.6034	3.7541	3.2742	2.6364	1.9530	1.2227	0.4229								15.8834	1.9854	1.8908
9	1.6827	3.9693	4.3719	3.9884	3.3734	2.6979	1.9922	1.2408	0.4264							20.2975	2.2553	1.9385
10	1.7053	4.2726	4.9422	4.6832	4.1081	3.4414	2.7456	2.0225	1.2543	0.4289						25.2338	2.5234	1.9586
11	1.7188	4.5207	5.4623	5.3511	4.8348	4.1845	3.4942	2.7843	2.0465	1.2646	0.4308					30.6916	2.7901	1.9577
12	1.7272	4.7215	5.9322	5.9871	5.5477	4.9248	4.2416	3.5378	2.8164	2.0660	1.2726	0.4323				36.6706	3.0559	1.9592
13	1.7328	4.8821	6.3534	6.5876	6.2419	5.6586	4.9881	4.2886	3.5751	2.8436	2.0819	1.2790	0.4334			43.1704	3.3208	1.9837
14	1.7368	5.0092	6.7286	7.1510	6.9133	6.3820	5.7317	5.0384	4.3291	3.6077	2.8667	2.0952	1.2842	0.4343		50.1909	3.5851	1.9947
15	1.7399	5.1086	7.0608	7.6765	7.5590	7.0915	6.4699	5.7869	5.0814	4.3652	3.6364	2.8867	2.1064	1.2885	0.4350	57.7320	3.8488	1.9945

Angular frequency, $\omega_{av,k}^{(max)}$ $(k = 1 \cdots 15)$, of the peak t.a.s.e. in lumped element Chebychev low-pass prototype filters.

degree	element 1	element 2	element 3	element 4	element 5	element 6	element 7	element 8	element 9	element 10	element 11	element 12	element 13	element 14	element 15	total t.a.s.e.
1	0.0000															0.0000
2	2.4181	-														2.0079
3	1.7949	1.3648	-													1.4986
4	1.5191	1.2909	1.1430	-												1.2900
5	1.3772	1.2228	1.1412	1.0669	-											1.1885
6	1.2950	1.1752	1.1210	1.0786	1.0343	-										1.1321
7	1.2438	1.1420	1.1020	1.0736	1.0475	1.0183	-									1.0976
8	1.2105	1.1182	1.0865	1.0656	1.0479	1.0303	1.0099	-								1.0750
9	1.1885	1.1006	1.0743	1.0579	1.0449	1.0328	1.0201	1.0051	-							1.0594
10	1.1739	1.0872	1.0646	1.0512	1.0410	1.0320	1.0232	1.0136	1.0023	-						1.0482
11	1.1643	1.0769	1.0568	1.0455	1.0372	1.0302	1.0236	1.0168	1.0094	1.0007	-					1.0399
12	1.1579	1.0687	1.0504	1.0407	1.0338	1.0280	1.0228	1.0177	1.0125	1.0066	0.9997	-				1.0335
13	1.1536	1.0622	1.0452	1.0367	1.0307	1.0259	1.0217	1.0177	1.0136	1.0094	1.0046	0.9991	-			1.0286
14	1.1505	1.0569	1.0409	1.0332	1.0280	1.0239	1.0204	1.0171	1.0139	1.0106	1.0071	1.0032	0.9987	-		1.0247
15	1.1482	1.0526	1.0373	1.0303	1.0256	1.0221	1.0190	1.0163	1.0137	1.0111	1.0084	1.0055	1.0022	0.9985	-	1.0215

Tolerance $< 1 * 10^{-4}$; LTA ratio: Largest to Average Ratio

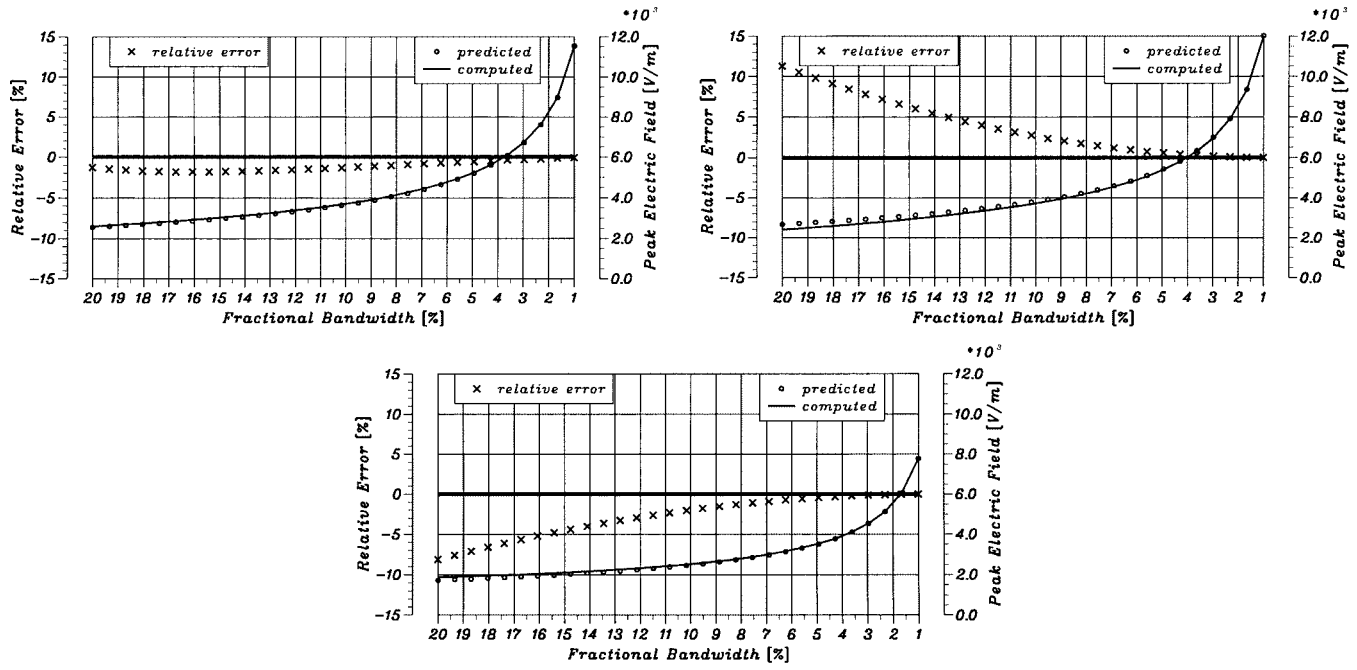

Fig. 3. Computed and predicted peak electric field strength (in kilovolts per meter) in the three cavities of third-degree Chebyshev direct-coupled-cavity filters with a minimum passband return loss of 20 dB, fractional bandwidths of $\Delta_{\rm BW} = 20\%, \ldots, 1\%$ and $f_{\rm center} = 1.586 f_c$. The passband center frequency, $f_{\rm center}$ of the filters was chosen to lie approximately in the center of the usable bandwidth of the $\rm TE_{10}$ mode, i.e., $f_{\rm center} \approx (1.25 + 1.90)/2 f_c = 1.575 f_c$. This corresponds approximately to a center frequency of 5 GHz ($1.586 f_c$) for a filter realization in WG12.

$\Delta_{\rm BW} = 20\%, \ldots, 1\%$, the computed and predicted peak electric-field strengths are shown in Fig. 3. This corresponds to a case when the relative error in (32) is large. Note that (32) becomes more accurate the more selective the filter is, i.e., (32) is more accurate for high-degree filters, narrow bandwidth filters, and filters with a low passband return loss than for low-degree filters, wide bandwidth filters, and filters with a large passband return loss. Several reasons account for this.

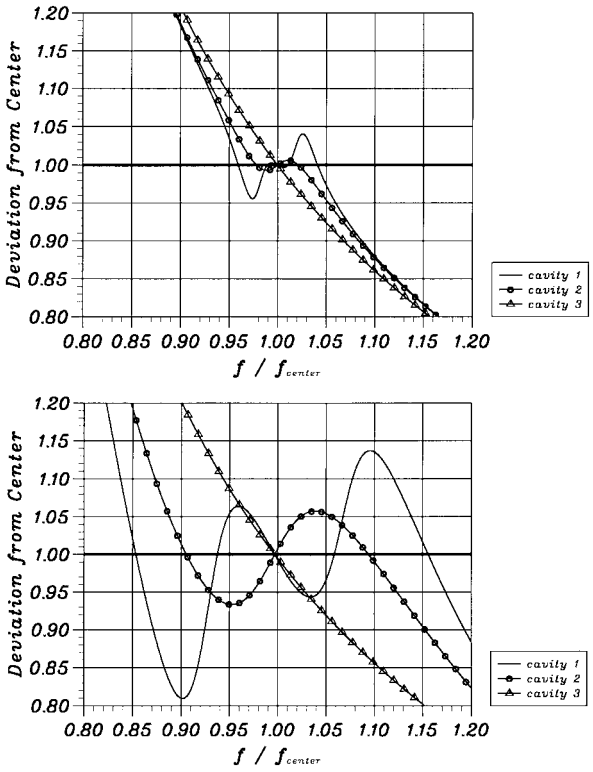

Fig. 4. Deviation $2z/\ell$ of the peak electric-field strength from the center of the cavity in 20% and 5% bandwidth transmission-line filter prototypes with 20-dB minimum passband return loss, three cavities, and $f_{\rm center} = 1.586 f_c$.

Firstly, the frequency transformation in (1) is of limited accuracy. It is derived from a narrow-band approximation of a transmission line [16]. Hence, a larger error is expected for wide-bandwidth filters than for narrow-bandwidth ones.

Apart from this systematic error, another source of error in (32) is the assumption that the peak electric-field strength occurs at the lower band edge of the passband. Again, however, this error is smaller in high selective filters than in low selective filters because the peak stored energy in a highly selective Chebyshev direct-coupled-cavity filter occurs closer to the band edges than in a less selective one (compare Tables I–III).

Also, in (32), it is implicitly assumed that the peak electric field occurs in the center of the cavity. It is well known that this is not the case. Khan [18] computed the voltages in the transmission-line model of TEM direct-coupled-cavity filters and was the first one who reported that the peak electric-field strength oscillates around the center position in the cavity with changing frequencies. This was also observed in this study and it was found that the amount of deviation depends on the bandwidth of the filter. In order to illustrate the variation in filters with different bandwidths, the computed deviation of the maximum field strength from the center location in the cavities is shown in Fig. 4 for some 20% and 5% fractional bandwidth Chebyshev direct-coupled-cavity filters with three cavities and 20-dB minimum passband return loss.

A. Conclusion

Equation (32) allows the prediction of the peak electric-field strength in a narrow-band transmission-line filter prototype of a direct-coupled-cavity waveguide filter to within a few percent accuracy from the stored energy analysis of the lumped-element low-pass prototype.

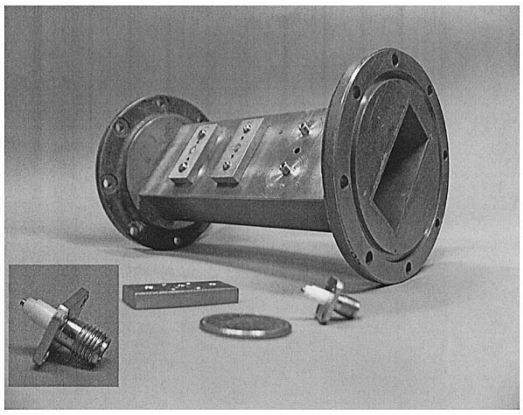

Fig. 5. Experimental waveguide filter and the coupling probe.

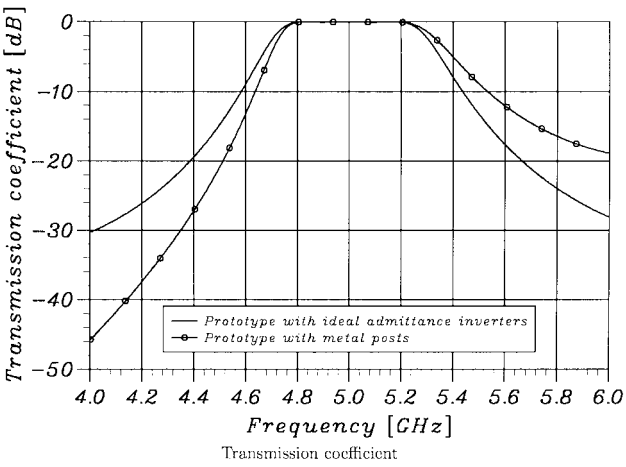

Fig. 6. Magnitude of the transmission coefficient in decibels of the filter prototype with ideal impedance inverters and the filter prototype with metal posts.

However, the transmission-line filter prototype is a purely $\rm TE_{10}$ mode model of a direct-coupled-cavity waveguide filter and it is assumed that the power coupling through the apertures is frequency independent. Also, dissipation loss is neglected. To investigate the effect of these factors, the peak electric-field strength in an experimental direct-coupled-cavity Chebyshev filter was measured and compared to a full-wave simulation of the structure (HP HFSS) and to the predicted peak electric-field strength obtained using (32).

IV. Prediction of the Peak Electric-Field Strength in a Third-Degree Direct-Coupled-Cavity Filter

A third-degree Chebyshev direct-coupled-cavity filter was designed in WG12 employing a design procedure similar to the one presented in [23]. The choice of the number of cavities ensured that the filter could be sufficiently accurately modeled on the workstation available using HP HFSS v. 5.1. A passband from $f_{\rm lo} = 4.8$ GHz to $f_{\rm hi} = 5.2$ GHz ($\Delta_{\rm BW} = 8\%$) was chosen with a minimum passband return loss of 20 dB. Any frequency band could have been chosen for the experimental filter, but a realization in WG12 has the advantage that the

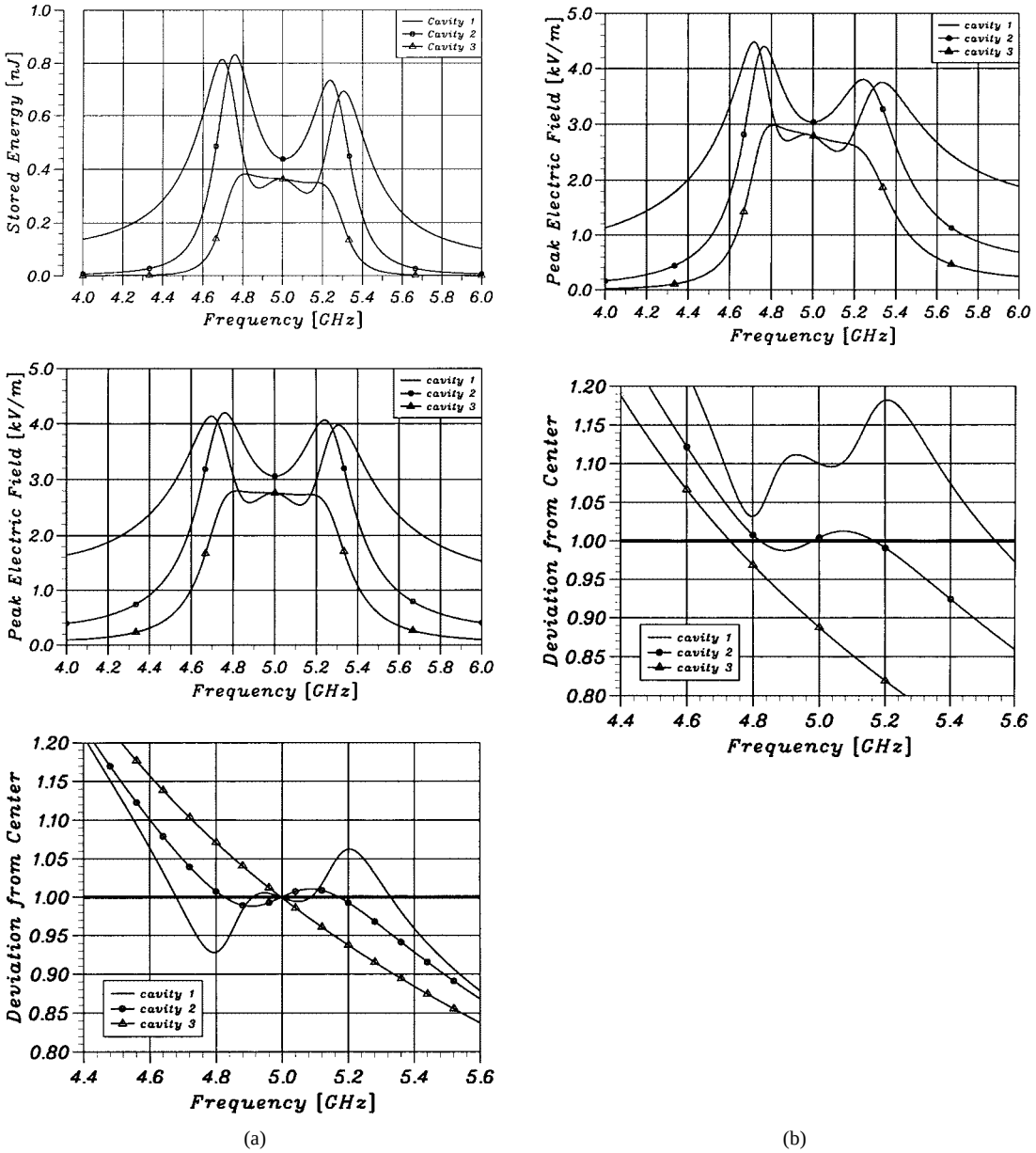

Fig. 7. Comparison of the peak electric-field strength, stored energy, and location of the maximum field in the transmission-line prototype filter with ideal impedance inverters with the transmission-line prototype with metal posts.

filter could be fabricated without the need of tuning, which is usually necessary due to fabrication tolerances. This is important since any tuning screw in a cavity would affect the field distribution in the cavity possibly to the extent that (32) is not valid anymore. Symmetrically located double posts were used to model the ideal impedance inverters in the transmission-line prototype. Operating at around 5 GHz also has the advantage that SMA connectors could be used as coupling probes into the cavities in order to measure the electric-field strength since their pin diameter is very small in comparison to the operating wavelength. A picture of the coupling probe that was used and the waveguide filter is shown in Fig. 5.

A. Predicted and Computed Results

When discontinuities, such as metal posts, are used to realize the ideal impedance inverters, the impedance inverter values become frequency dependent [17]. This affects the return- and insertion-loss function. The reflection zeros in the passband are slightly shifted down in frequency and the insertion loss increases in the lower stopband and decreases in the upper stopband, as observed in Fig. 6. Hence, it is expected that the peak electric-field strength on the lower side of the passband is larger in the prototype with metal posts than in the one with ideal impedance inverters. This agrees with the graphs of the peak electric-field strength in Fig. 7 where the total stored energy, peak electric-field strength, and location of the peak electric-field strength with respect to the center of the cavities is plotted for both prototype filters.

Note that the deviation from the center of the cavity of the peak electric-field strength in the filter with metal posts is different to the one with ideal impedance inverters since the negative lengths of line needed to embed the metal posts to realize

TABLE IV
PREDICTED, COMPUTED, MEASURED, AND SIMULATED PEAK ELECTRIC-FIELD STRENGTH CORRESPONDING TO THE CASE WHEN THE EXPERIMENTAL FILTER IS DRIVEN BY A GENERATOR WITH 1-W AVAILABLE POWER

	Equation (32) (Based on filter with ideal impedance inverters)	Computed (Filter with ideal impedance inverters)	Computed (Filter with physical model of metal posts)	Simulated (HP-HFSS)	Measured
$\mathbf{E}_{max,1}$	4.099	4.140	4.485	4.724	4.591
$\mathbf{E}_{max,2}$	4.269	4.200	4.403	4.613	4.506
$\mathbf{E}_{max,3}$	2.764	2.799	2.985	3.153	3.114

Peak electric field strength in $\frac{kV}{m}$

	Equation (32)	Computed	Computed	Simulated	Measured
$f_{max,1}$	4.800	4.697	4.716	4.710	4.712
$f_{max,2}$	4.800	4.760	4.764	4.760	4.754
$f_{max,3}$	4.800	4.819	4.805	4.800	4.798

Frequency in GHz at which the peak electric field strength occurs

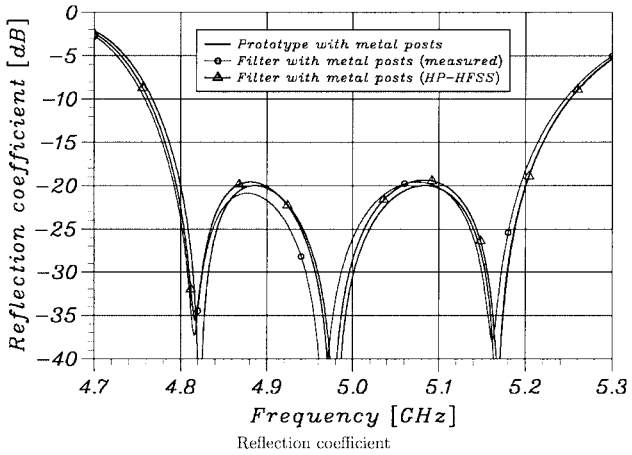

Fig. 8. Computed, simulated, and measured filter response.

the impedance inverters [1] have been absorbed into the cavities. This offsets the location of the electrical center of the cavities in the filter with metal posts in comparison to the filter with ideal impedance inverters. Only the electrical center of the middle cavity is unchanged because the filter is physically symmetrical.

The peak electric-field strengths in the three cavities have been listed in Table IV, including the peak electric-field strengths predicted by (32). The peak stored energies in a 20-dB lumped low-pass prototype filter was used for the evaluation of (32), i.e., $\max\{W_{\mathrm{av},1}\} = 0.9387$, $\max\{W_{\mathrm{av},2}\} = 1.0180$, and $\max\{W_{\mathrm{av},3}\} = 0.4267$.

B. Results From HFSS

The reflection coefficient computed by HP HFSS and the one obtained from the transmission-line prototype with metal posts is shown in Fig. 8. Very close agreement is observed. A wide-band frequency sweep of the transmission coefficient showed excellent agreement between the transmission coefficient computed by HP HFSS, the transmission coefficient of the filter prototype with metal posts, and the measured transmission coefficient.

Solving the EM field for frequencies around the lower band edge, the peak electric-field strength in the three cavities was determined and has been collected as shown in Table IV. Close agreement with the peak electric-field strength in the prototype with metal posts can be observed (less than 6% deviation).

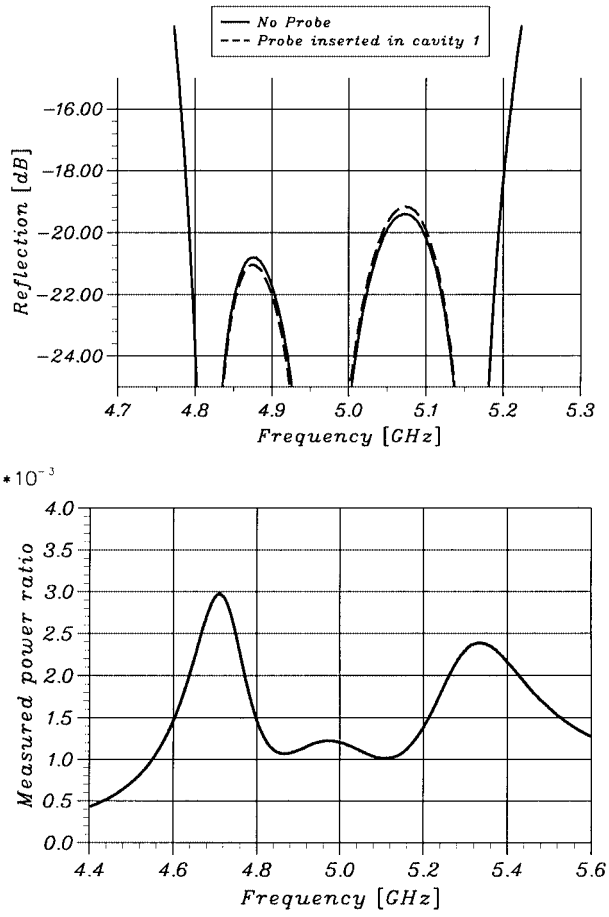

Fig. 9. Measured results probing into the first cavity.

C. Measured Results

The electric-field strength in the experimental filter was measured employing principles that were commonly used to measure the voltage standing-wave ratio (VSWR) using

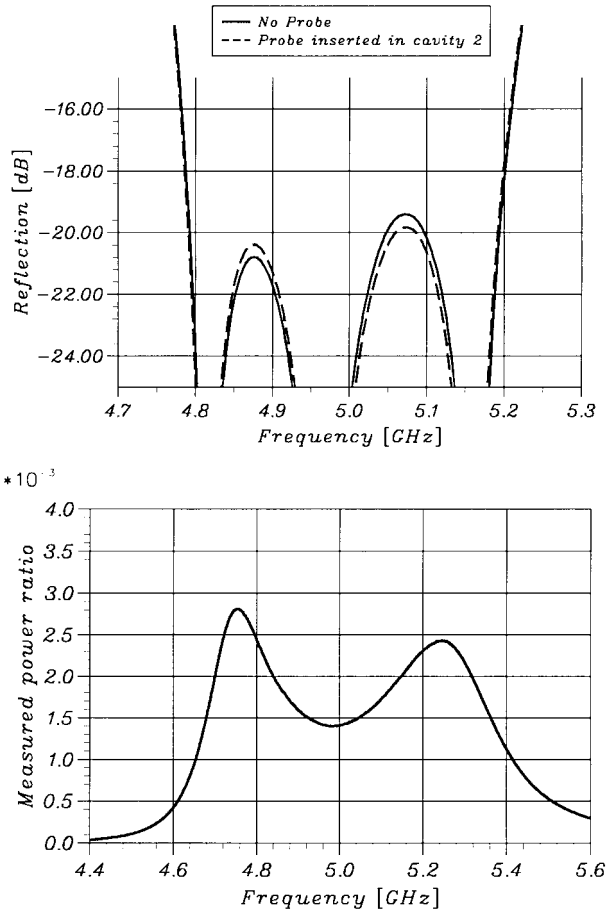

Fig. 10. Measured results probing into the second cavity.

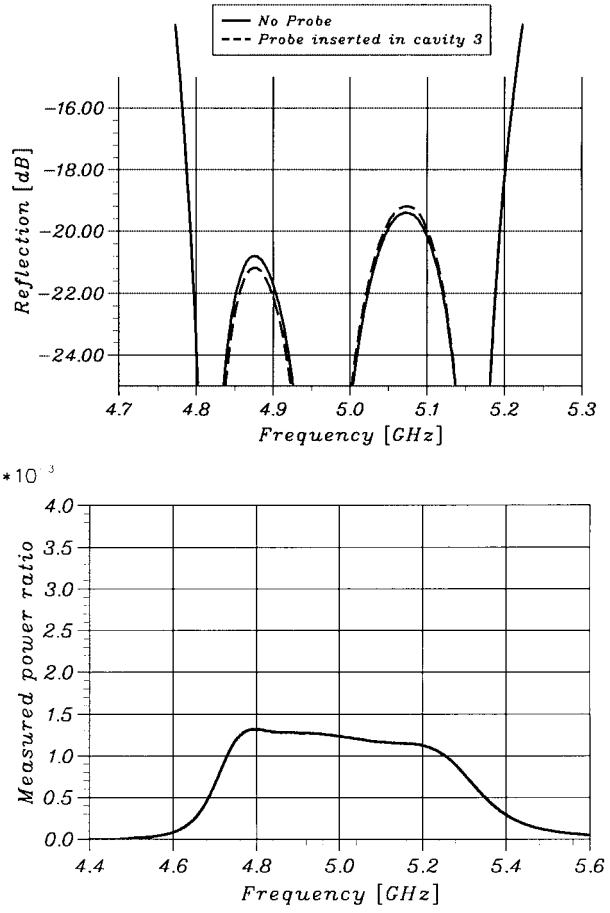

Fig. 11. Measured results probing into the third cavity.

a slotted waveguide and a crystal detector [24]. In Fig. 5, it is shown how probes were introduced into the waveguide cavities. An SMA connector acting as a probe was centered onto the top wall of a cavity and connected to a network analyzer. The measured power transmission through the coupling aperture when probes are inserted into the cavities is shown in Figs. 9(b)–11(b), respectively. Even though it is not possible to incorporate the coaxial-to-rectangular waveguide transition in the calibration, the shape of the measured power transmission through the probes is very similar to the computed peak stored energy. This is due to the high quality of the coaxial-to-waveguide transition that was used.

Only very little power is coupled out of the filter through the probes. Still it affected the filter performance, as observed in Figs. 9(a)–11(a). However, the effect on the measurement accuracy is estimated to be very small since the selectivity of the filter is hardly changed. Relating the measured power by the network analyzer to a known electric-field strength at the probe location, the measured power can then be directly related to the electric-field strength at the position of the probe. Three simple short-circuited stubs were used with the same coupling hole as in the waveguide filter located a quarter-wavelength away from the short-circuited end at the frequencies 4.67, 4.80. and 5.00 GHz. The calculated peak electric-field strengths in the three cavities are 4.591, 4.506, and 3.114 kV/m, respectively. This agrees to within 10% with the predicted ones using (32).

D. Comparison of Predicted, Computed, Simulated, and Measured Results

In Table IV, the peak electric-field strengths in the cavities of the experimental filter are listed. It includes the measured peak electric-field strengths, the predicted ones using (32), the simulated ones using a full-wave structure simulator (HP HFSS), and the computed ones in two different types of transmission-line prototype filters. Equation (32) predicts very accurately the peak t.a.s.e. in the prototype with ideal impedance inverters. However, in reality, the couplings are frequency dependent. This is the main reason of the observed deviation of approximately 10% of (32) from the measured data.

V. Conclusion

An explicit expression for the peak internal fields in the cavities of direct-coupled rectangular waveguide cavity filters has been derived. Comparison with HP HFSS simulations and measurements of a test filter has demonstrated the good accuracy of the expression obtained. This expression is very useful in the analysis and study of the power-handling capability of these types of filters as, together with the provided tables of the peak stored energy in commonly used Chebyshev lumped-element prototype filters, the peak electric-field strength in direct-coupled rectangular waveguide cavity filters are now easily computed.

The procedure presented here for a rectangular waveguide can equally be applied to any type of resonator and excited mode if the field distribution in the resonator is known at resonance. Some consideration has already been given to combine filters [25].

In this paper, explicit consideration has been given to the case of direct-coupled-cavity filters. Similar principles apply to multiple-coupled-cavity filters, where, again, the peak internal field can be related to the peak t.a.s.e. in the lumped low-pass prototype from which it is derived.

The accuracy of the expressions derived in this paper may be further improved by employing a more accurate frequency transformation [17] that also takes into account the frequency dependency of the coupling apertures.

REFERENCES

[1] G. L. Matthaei, L. Young, and E. M. T. Jones, *Microwave Filters, Impedance-Matching Networks and Coupling Structures*. Dedham, MA: Artech House, 1964.

[2] S. B. Cohn, "Design considerations for high-power microwave filters," *IRE Trans. Microwave Theory Tech.*, vol. MTT-7, pp. 149–153, Jan. 1959.

[3] C. Kudsia, R. Cameron, and W. C. Tang, "Innovations in microwave filters and multiplexing networks for communications satellite systems," *IEEE Trans. Microwave Theory Tech.*, vol. 40, pp. 1133–1149, June 1992.

[4] A. D. MacDonald, *Microwave Breakdown in Gases*. New York: Wiley, 1966.

[5] *Multipactor, RF and DC Corona and Passive Intermodulation in Space RF Hardware*. Noordwijk, The Netherlands: European Space Agency, 2000, Workshop Proc. WPP-178 .

[6] L. Young, "Peak internal fields in direct-coupled-cavity filters," *IRE Trans. Microwave Theory Tech.*, vol. MTT-8, pp. 612–616, Nov. 1960.

[7] C. Ernst and V. Postoyalko, "Comparison of the stored energy distribution in a QC-type and a TC-type prototype with the same power transfer function," in *IEEE MTT-S Int. Microwave Symp. Dig.*, 1999, pp. 1339–1342.

[8] C. Ernst, V. Postoyalko, and R. Parry, "Energy distributions in different filter realizations with the same power transfer function," in *Microwave Filters and Multiplexers*. London, U.K.: IEE Press, 2000, IEE Seminar 00/117, pp. 9/1–9/15.

[9] C. Ernst, V. Postoyalko, R. Parry, and I. Hunter, "Filter topologies with minimum peak stored energy," in *IEEE MTT-S Int. Microwave Symp. Dig.*, Phoenix, AZ, May 2000, pp. 1631–1634.

[10] C. Ernst, "Energy storage in microwave cavity filter networks," Ph.D. dissertation, School Electron. Elect. Eng., Univ. Leeds, Leeds, U.K., 2000.

[11] H. J. Carlin, "Network theory without circuit elements," *Proc. IEEE*, vol. 55, pp. 482–497, 1967.

[12] P. P. Penfield, R. Spence, and S. Duinker, *Tellegen's Theorem and Electrical Networks*, ser. Res. Monograph 58. Cambridge, MA: MIT Press, 1970.

[13] C. Ernst, V. Postoyalko, and N. Khan, "The relationship between group delay and stored energy in microwave filter networks," *IEEE Trans. Microwave Theory Tech.*, vol. 49, pp. 192–196, Jan. 2001.

[14] S. B. Cohn, "Direct-coupled-resonator filters," *Proc. IRE*, pp. 187–196, Feb. 1957.

[15] M. Yu and A. Sivadas, "A simplified analysis for high power microwave bandpass filter structures," in *Multipactor, RF and DC Corona and Passive Intermodulation in Space RF Hardware*. Noordwijk, The Netherlands: European Space Agency, 2000, Workshop Proc. WPP-178 .

[16] R. Levy, "Theory of direct-coupled-cavity filters," *IEEE Trans. Microwave Theory Tech.*, pp. 340–348, June 1967.

[17] J. D. Rhodes, "The generalized direct-coupled cavity linear phase filter," *IEEE Trans. Microwave Theory Tech.*, vol. MTT-18, pp. 308–313, June 1970.

[18] N. G. Khan, "High power microwave filters," Ph.D. dissertation, School Electron. Elect. Eng., Univ. Leeds, Leeds, U.K., Nov. 1997.

[19] R. E. Collin, *Foundations for Microwave Engineers*, 2nd ed. New York: McGraw-Hill, 1992.

[20] J. Schwinger and D. S. Saxon, *Documents on Modern Physics: Discontinuities in Waveguides (Notes on Lectures by Julian Schwinger)*. New York: Gordon and Breach, 1948.

[21] E. A. Guillemin, *Synthesis of Passive Networks*. New York: Wiley, 1957.

[22] J. D. Rhodes, *Theory of Electrical Filters*. New York: Wiley, 1976.

[23] V. Postoyalko and D. S. Budimir, "Design of waveguide E-plane filters with all-metal inserts by equi-ripple optimization," *IEEE Trans. Microwave Theory Tech.*, vol. 42, pp. 217–222, Feb. 1994.

[24] C. G. Montgomery, *Technique of Microwave Measurements*. Englewood Cliffs, NJ: McGraw-Hill, 1947.

[25] A. R. Harish and R. J. Cameron, "Peak voltage analysis in high power microwave filters," in *Microwave Filters and Multiplexers*. London, U.K.: IEE Press, 2000, IEE Seminar 00/117, pp. 10/1–10/5.

Christoph Ernst (S'96–A'00) was born in Loerrach, Germany. He received the Dipl.-Ing. degree in electrical engineering from the University of Dortmund, Dortmund, Germany, in 1996, and the Ph.D. degree in electronic and electrical engineering from the Institute of Microwaves and Photonics, The University of Leeds, Leeds, U.K., in 2001. His doctoral dissertation concerned the optimization of the power-handling capability of microwave filters.

His current field of research is the design of microwave circuits.

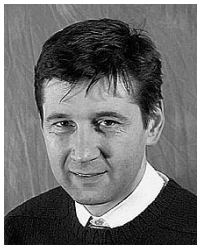

Vasil Postoyalko (S'82–M'82) was born in Leeds, U.K. He received the B.Sc. degree in mathematics and the Ph.D. degree in electronic engineering and applied mathematics from The University of Leeds, Leeds, U.K., in 1978 and 1985, respectively.

In 1983, he became a Research Engineer with the School of Electronic and Electrical Engineering, The University of Leeds, and since 1986, he has been a Lecturer. He is a member of the Institute of Microwaves and Photonics, The University of Leeds. His current research interest is in the design of microwave circuits.